

# Numerical Analysis of Two Hyperloop Pods

Mohammad Islayem <sup>a</sup>, Mohammed Tarnini <sup>a</sup>, Isam Janajreh <sup>a\*</sup>

<sup>a</sup> Department of Mechanical Engineering, Khalifa University of Science and Technology, Abu Dhabi, UAE

## Abstract

Hyperloop is forecasted to be the future transportation system for medium distance range. It consists of levitated pods traveling inside a reduced pressure tunnel/tube near the transonic speed. The flow around the pod is limited to Mach speed to avoid the choking and shockwaves formation that can cause damages and destabilization of the pod and the tube. The most crucial parameter in the hyperloop traveling system is the aerodynamic drag. In this study, numerical flow simulation of compressible steady air flow has been done on the hyperloop pod traveling inside the low-pressure tunnel environment. Two-dimensional axisymmetric simulations were carried out to assess the flow and aerodynamic forces exerted on the pods under varying speed (25 to 350 m/s) and separation distance (10.75, 21.5, 43, 86 m) between two pods. For all the cases, Mach number =1 flow speed is reached at a value between 150 to 200 m/s and the shockwaves start appearing on the 2<sup>nd</sup> pod at a value between 200 to 250 m/s. Results show that shockwave appeared at the 1<sup>st</sup> pod at separation distance of 86 m and speed 350 m/s. Overall, the pressure drag has more impact on the total drag than the friction drag especially at the 2<sup>nd</sup> pod. The total drag obtained at the 1<sup>st</sup> pod in a multiple pod model is less than the total drag in a single pod model, while it is higher at the 2<sup>nd</sup> pod when compared with a single pod model.

**Keywords:** Hyperloop, Multiple pods, Steady flow, Drag coefficients

## 1. Introduction

The Hyperloop concept, which was strongly advocated by Musk in 2013, is a new transportation system that thought to enhance transportation by reducing traveling time [1, 2]. It has been of considerable interest lately to enhance the transportation system, especially for medium and long-distance trips avoiding airports congestions and delays and being less sensitive to adverse weather conditions. The performance of the Hyperloop can be affected by changing several parameters like blockage ratio (BR), pod length, head and tail shapes, pressure inside the tube, and speed of the pod [3]. Le and coworkers studied the motion of a hyperloop pod and propagation of pressure waves [4]. The speed of the pod was changed from 100 m/s to 350 m/s, and the authors reported that the drag coefficient ( $C_D$ ) is increased as BR, pod length, and pod speed are increased [4]. It was also recorded that the propagation speed of the expansion waves was close to the speed of sound, while the propagation speed of the compression waves was much higher than the speed of sound [4]. Niu et al. stated that a high pod speed at high blockage ratio increases the temperature inside the tube and dramatically changes the pressure which compromise the safety of the body

of the pod [5]. The results of studying the formation of heating and the effect of having the pod move at subsonic, transonic, and supersonic speeds showed that there is formation of shockwaves at the front and the back of the pod, where properties like temperature and pressure greatly change due to the shockwave [5]. Wang et al. confirmed that at low pod speeds the relationship between aerodynamic drag and BR is linear, but became non-linear at high pod speeds [6]. Moreover, Ma et al. found that the aerodynamic drag on the pod is proportional to the square of the pod speed and the air pressure inside the tube [7]. Mao et al. studied the effects of changing the vacuum levels with the heat dissipation from magnetically levitated pods at high speeds [8]. The results showed that with the decrease of vacuum levels from 101.325 kPa to 10.1325 kPa, the heat dissipating from the pod is decreased by 49% after 60 minutes [8]. Le et al. performed numerical simulations on hyperloop pods with upward tails and downward tails while also changing the length of the downward tail from 1.725 m to 13.8 m [9]. It was concluded that the tail shapes of the pod do not have a major effect on the pod aerodynamic performance, where there is only a 0.75% difference between the downward and upward tails [9]. The increase of the tail length causes the aerodynamic drag to decrease by approximately 7% [9]. The flow fields at the rear of the pod and around it were massively affected by the increase in tail length [9].

\* Corresponding author. Tel.: +971 2 312 3286

Fax: +971 2 312 3286; E-mail: isam.janajreh@ku.ac.ae

© 2016 International Association for Sharing Knowledge and Sustainability

DOI: 10.5383/ijtee.19.02.002

Bose et al. studied the effect of adding aerofoil-shaped fins to the aeroshell on the hyperloop surface [10]. A 3D analysis was conducted on a hyperloop pod inside a vacuum tube and the results showed that the addition of the fins caused a reduction in the drag and the pressure in front of the pod [10]. Rodriguez et al. studied the effect of installing a compressor in front of the pod on the hyperloop performance [11]. The results showed adding a compressor at higher speed has a huge impact on the performance. For example, at 194 m/s the blockage ratio can reach as high as 0.5 to 0.6 compared to only 0.18 without the compressor. This signifies that for a fixed pod diameter, the tube diameter can be substantially decreased [11]. Hu et al. studied the effect of inserting cross passage inside the tunnel [12]. The results obtained showed that the highest decrease in the aerodynamic drag occurs when the head car's nose tip enters the cross passage [12].

Nick et al. studied two different designs for the hyperloop, i.e., the short and the optimized. The short design was made to delay the transition from laminar to turbulent, hence, decreasing the frictional drag, and the optimized design was made by decreasing the area in front of the pod to make the transition occurs near the front [13]. Their results showed that drag decreases by 14% when using the optimized model where the area in the front decreased [13]. A study made by Le et al. focused on testing the effects of increasing the number of pods on the aerodynamic drag by varying the pod speed and the separation distance between the pods [14]. The results obtained showed that at lower speed (100 m/s) the length between the pods almost do not affect the average aerodynamic drag nor do the number of pods [14]. At 200 m/s, increasing the number of pods and their clearance distance slightly decreases the average drag [14]. At 300 m/s, adding more pods especially if they are connected has a relatively large impact on decreasing the average drag [14].

The above review insight one to investigate further the role of pod velocity on the drag force for two pods arrangement. In this paper, two hyperloop pods will be analyzed by varying their traveling speed and the distance between the pods from 25 to 350 m/s and from 10.75 to 86 m, respectively. The pressure drag, viscous drag, maximum Mach number of the flow, and the maximum pressure inside the tube will be analyzed. The remaining sections of the paper are organized as follows: Section 2 consists of the methodology that was utilized to carry out the study. In Section 3, presenting and discussing the results obtained from the study. In Section 4 the conclusions of the work will be drawn.

## 2. Methodology

This section will provide the detailed numerical setup used to run the needed simulations, including the assumptions made, the computational model setup, and its boundary conditions following computational fluid dynamic (CFD) simulation.

The flow is assumed to be viscous, steady-state, and compressible. The tube and the pod surfaces are assumed to be smooth. A 2-dimensional axisymmetric numerical domain is considered, taking advantages of the tubular roundness, to

reduce the total discretization cells and the overall “degree of freedom” associated with the unknown dependent variables, i.e., velocities, pressure, density, temperature, and turbulent scalars. Oh et al. [3] studied the difference between the results obtained from 2D axisymmetric model and 3D model, and stated that the difference is within 4% discrepancies. Since the flow includes both laminar and turbulence regions, the Transition Shear-Stress Transport (Transition SST) viscous model is used which was proven to be a suitable model for this study.

Fig. 1 illustrates the computational geometry used for the multiple hyperloop system. The lengths of the tube and the pod 360 m and 43 m, respectively, with pod diameter of 3 m and tube of 5 m. This stretching the 2D-axisymmetric model 360m axially and 2.5 m radially. The domain can be then mirrored at the axis to give 3 and 5 m diameter of pod and tube, respectively.

The discretized grid is generated with quadratic elements type using ANSYS preprocessor. The boundary conditions were set to be pressure far-field at the inlet, where the speed and the pressure of the flow entering the tube can be controlled. Also, pressure outlet condition was applied at the outlet of the tube. The walls of the tube were set to be moving with the same speed as the inlet, and the walls of the pod were stationary walls. Moreover, the bottom edge of the numerical domain is considered an axis of axisymmetric, and the results can be mirrored around the axis to get the complete flow picture.

The governing flow system are those equations including the continuity (Eq. 1), momentum (Eq. 2), and energy (Eq. 3) conservation equation. These in of unsteady flow are written as:

$$\frac{\partial \rho}{\partial t} + \frac{\partial(\rho u_i)}{\partial(x_i)} = 0 \quad (1)$$

$$\frac{\partial(\rho u_i)}{\partial t} + \frac{\partial(\rho u_i u_j)}{\partial(x_j)} = -\frac{\partial P}{\partial x_i} + \frac{\partial}{\partial x_j} \left[ \mu \left( \frac{\partial u_i}{\partial x_j} + \frac{\partial u_j}{\partial x_i} - \frac{2\delta_{ij}}{3} \frac{\partial u_k}{\partial x_k} \right) \right] + \frac{\partial}{\partial x_j} (-\rho \{u_i u_j\}) \quad (2)$$

$$\frac{\partial(\rho E)}{\partial t} + \frac{\partial}{\partial x_j} (u_j(\rho E + P)) = \frac{\partial}{\partial x_j} \left[ (k_{eff}) \frac{\partial T}{\partial x_j} \right] + \frac{\partial}{\partial x_j} \left[ u_i \mu_{eff} \left( \frac{\partial u_i}{\partial x_j} + \frac{\partial u_j}{\partial x_i} - \frac{2\delta_{ij}}{3} \frac{\partial u_k}{\partial x_k} \right) \right] \quad (3)$$

Where  $\rho$  is the air density,  $u$  is the flow velocity,  $P$  is the pressure,  $E$  is the specific internal energy,  $k_{eff}$  is the effective thermal conductivity, and  $\mu_{eff}$  is the effective dynamic viscosity. The  $BR$  is the ratio between the area of the pod and the area of the tube, which is given by the relation:

$$BR = \frac{A_{pod}}{A_{tube}} \quad (4)$$

Where  $A_{pod}$  is the cross-sectional area of the pod and  $A_{tube}$  is the cross-sectional are of the tube. For a certain  $BR$  value, there is a maximum pod speed that can be reached before the

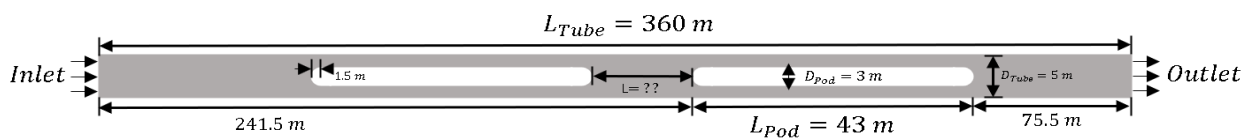


Fig. 1: Computational Model Schematic showing the considered lengths and diameters for the tube and the pod

onset of chocking around the pod [15]. Kantrowitz limit provides a relation between the BR and the maximum pod speed, where the relation is expressed as follow:

$$BR = 1 - Ma \left( \frac{1 + \frac{\gamma-1}{2} Ma^2}{1 + \frac{\gamma-1}{2} Ma^2} \right)^{\frac{\gamma+1}{2(\gamma-1)}} \quad (5)$$

Where Ma is the pod speed expressed as Mach number and  $\gamma$  is the specific heat ratio for the air.

Grid sensitivity test was done to assess the accuracy of the developed numerical model. Therefore, five different grids were generated as shown in Table 1. For each grid, the error was calculated based on the total drag and the maximum pressure based on the finest grid labeled as Fine 2 in Table 1 that comprises 436,197 cells. The error obtained for the baseline grid is 2.39% and 1.01% for the total drag and the maximum pressure, respectively. This baseline grid is chosen for the current simulations as trade of between accuracy and computational cost.

**Table 1: Grid Sensitivity Test**

| Case     | Number of Nodes | Total Drag       | Max Pressure   |
|----------|-----------------|------------------|----------------|
| Coarse 1 | 36,983          | 1484.12 (11.31%) | 281.11 (3.86%) |
| Coarse 2 | 70,685          | 1371.15 (2.84%)  | 260.24 (3.85%) |
| Baseline | 132,636         | 1365.2 (2.39%)   | 267.93 (1.01%) |
| Fine 1   | 224,367         | 1334.5 (0.092%)  | 265.61 (1.87%) |
| Fine 2   | 436,197         | 1333.27          | 270.67         |

### 3. Results and Discussion

The hyperloop system has several main parameters like BR, pod speed, pod length, head and tail shapes, and tube pressure. Simulations were done using a wide range of parameter settings to enable a thorough investigation of the drag on the pod. The speed of the pod was varied from 25 to 350 m/s, and the distance between the pods was varied from 0.25L to 2L (10.75-86 m). Furthermore, the pressure inside the tube was maintained at 101.325 Pa and the temperature at 300 K. The pressure drag at the pod surface is affected by the flow separation and body shape of the pod. Moreover, the friction drag is influenced by the properties of the boundary layer like viscosity, Re, and surface roughness. The pressure drag, friction drag, and total drag were recorded at each pod speed while changing the distance between pods. The goal is to investigate the effects of pressure drag, and friction drag on two pods under variable pod speed and clearance distance between the pods.

#### 3.1. Mach number analysis

The presence of choke flow of the fluid inside the tube is related to the BR and Mach number of the pod. The BR is fixed at 0.36 in all simulations, so the speed of the pod will be varied to see at what speed the choke flow occurs. The pod speeds were swept over 25, 50, 100, 150, 200, 250, 300, and 350 m/s range. **Error! Reference source not found.** shows the contours of Mach number of the fluid when changing the pod speed, where the pods are separated by 2L distance (86 m) from each other. It is seen that the Mach number of the fluid keeps increasing with increasing pod speeds. The Mach number reaches its maximum value specifically near the confined spaces around the pods. At pod speed = 150 m/s, the Mach number of the fluid is 0.72, while at pod speed = 200 m/s, the Mach number reached 1.09. This means that the critical pod speed value where the Mach number of the fluid is exactly 1 Mach number is between 150 m/s and 200 m/s. According to Oh et al. [3], the analysis on single pod under the same conditions showed that the critical pod speed

value is 180 m/s. It is also noticeable that the maximum Mach number increases massively at pod speeds 200 to 250 m/s, which is due to the formation of shockwaves at the 2<sup>nd</sup> pod. To further analyze the Mach number of the fluid around the pods, the distance between the pods was decreased. The new employed distances were 1L, 0.5L, and 0.25L (43, 21.5, and 10.75 m), respectively. The results obtained showed similar trends of increasing Mach number with increase of pod speed across all distances. The critical pod speed was also between 150 m/s to 200 m/s. Furthermore, there were shockwaves formed at speeds equal to and greater than 250 m/s. The only difference that occurred while varying the distance is that at distance of 2L between the pods, shockwaves were formed at the 1<sup>st</sup> pod when pod speed was 350 m/s. This phenomenon did not occur in any other case where it could have happened due to the high-pressure region between the pods.

#### 3.2. Static pressure analysis

The static pressure of the fluid inside the tube was also studied under the same conditions as the analysis of Mach number where pod speed was changed from 25 to 350 m/s. As shown in Fig. 2, it is seen that as the pod moves faster, the maximum pressure increases. It is clear from the contours that the pods compress the air in the upstream creating a high-pressure region. This means that the 1<sup>st</sup> pod is became subjected to high pressure regions in the upstream and downstream. This could have been the reason of the delay of shockwave formation as it was seen from the Mach number contours. The maximum pressure at pod speed = 350 m/s is 238.2 Pa which is more than double the pressure at the inlet. At 200 m/s which is extremely close to the critical pod speed, the maximum pressure reached is 149.51 Pa. In contrast to the Mach number contour, there was no sudden increase in static pressure at pod speed 250 m/s as there was in Mach number. However, it is noticed that at pod speeds 250 and 300 m/s, the maximum pressure region is in the upstream and downstream of the 1<sup>st</sup> pod rather than in the upstream only for the other pod speeds. The low-pressure region that is developed due to the shockwaves can be clearly seen behind the 2<sup>nd</sup> pod at speeds 250, 300, and 350 m/s. This low-pressure region is also observed in the downstream of the 1<sup>st</sup> pod at speed 350 m/s. The distance between the pods was reduced to 1L, 0.5L, and 0.25L, and the simulations were repeated. The low-pressure region due to shockwaves at the 1<sup>st</sup> pod did not occur in any of the other cases. This means that there is a certain distance between the pods where shockwaves start to develop at the 1<sup>st</sup> pod.

#### 3.3. Drag forces

The drag forces at both pods were investigated while increasing the pod speeds from 25 to 350 m/s, and the distance between the pods from 0.25L to 2L. Fig. 4 presents the effect of speed and distance changes on the pressure drag at the surface of the two pods. At pod 1, the pressure drags did not significantly change when speed increased as well as the distances for 0.25L, 0.5L, and 1L. The pressure drag forces for these three cases were around 200 N and below at all speeds. These low pressure drags are expected because there is a high-pressure region in the upstream and downstream of 1<sup>st</sup> pod. However, for the case of 2L distance between the pods, the pressure drags at 1<sup>st</sup> pod increased massively and reached about 1100 N at pod speed of 350 m/s. This increase in pressure drag is due to the formation of shockwaves where low pressure region was created at the downstream of 1<sup>st</sup> pod. The difference between the high pressure in the upstream of 1<sup>st</sup> pod and the low pressure in the downstream is what

created this spike in pressure drag. As for 2<sup>nd</sup> pod, the pressure drag trend was similar for all cases where the pressure drags kept increasing as speed was increasing and at a higher rate when the pod speed was between 200 and 250 m/s where shockwaves started to form. The pressure drags at 2<sup>nd</sup> pod reached around 1200 N at pod speed of 350 m/s for the three cases of 0.25L, 0.5L, and 1L. The pressure drag decreased slightly at speed 350 m/s because of the shockwave formation at 1<sup>st</sup> pod which decreases the pressure at the region between pods.

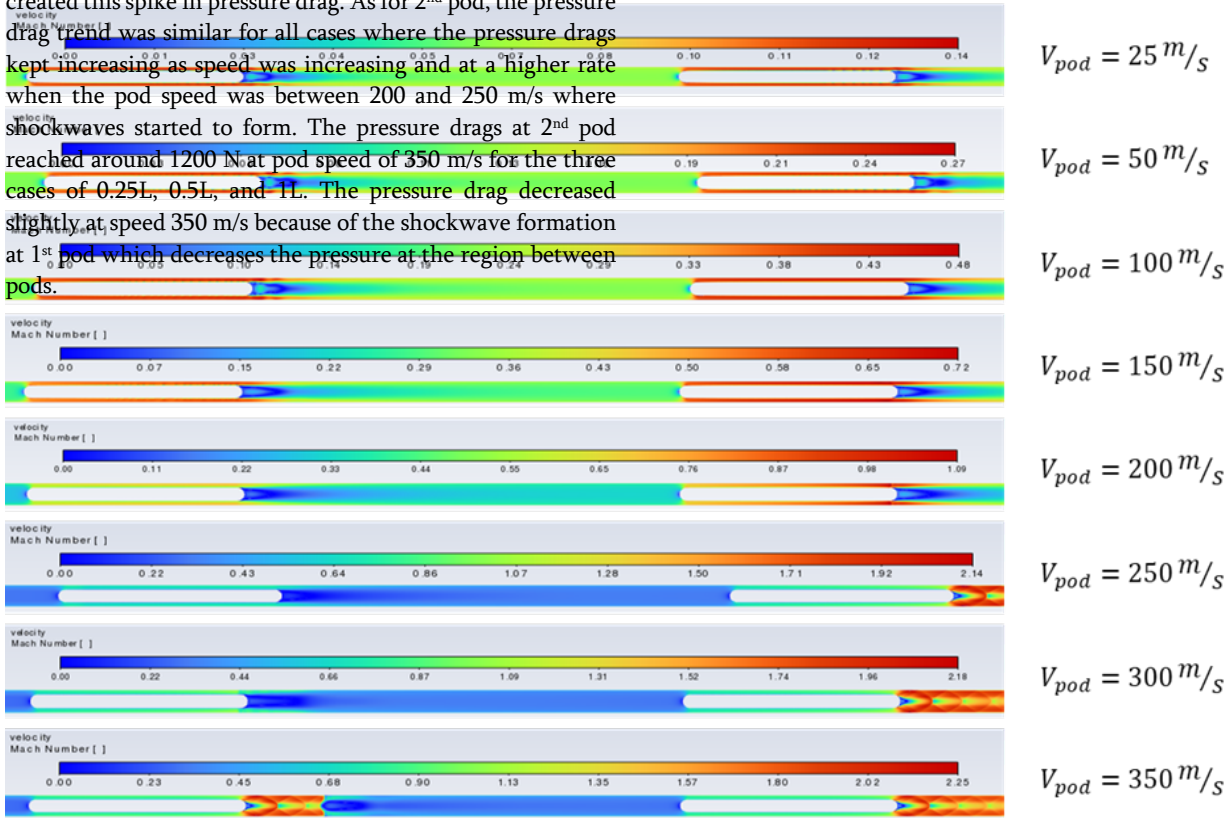


Fig. 2: Contours of Mach number of the fluid inside the tube for various pod speeds at 2L distance

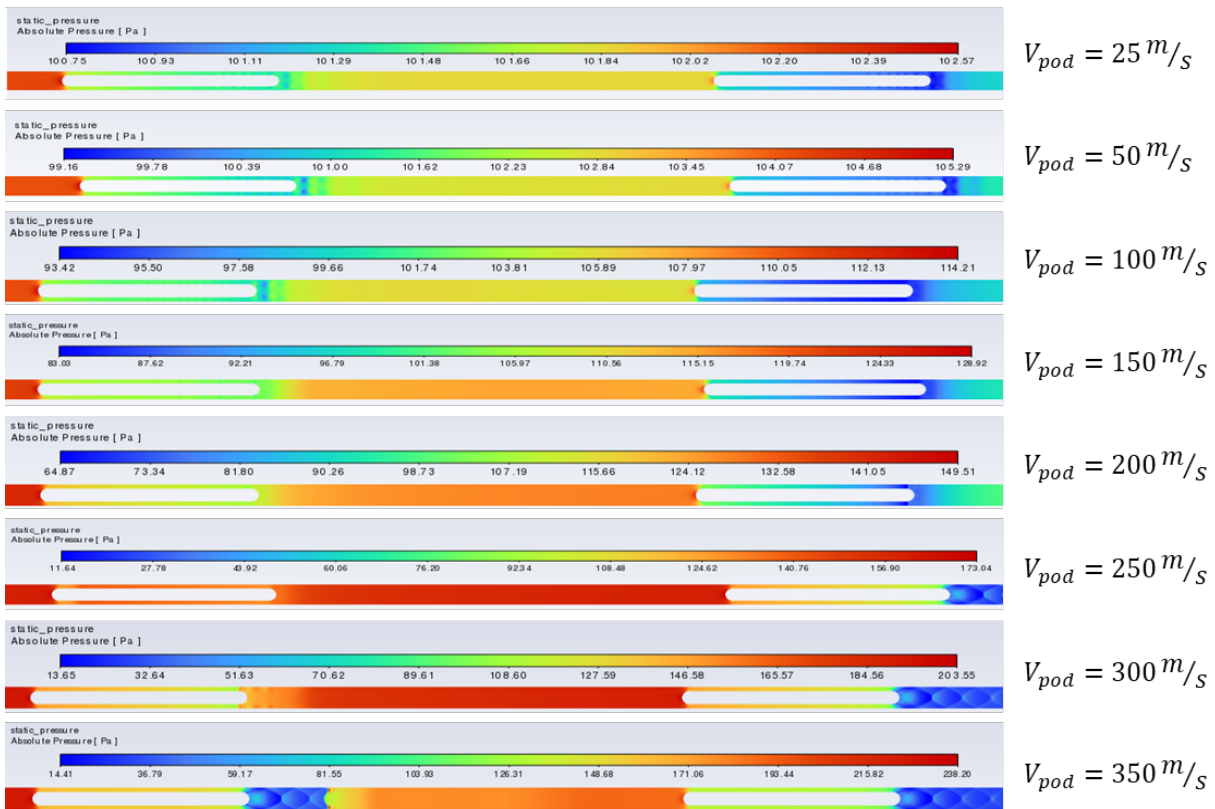


Fig. 3: Contours of static pressure of the fluid inside the tube for various pod speeds at 2L distance

The difference of pressure magnitude in the upstream and downstream of 2<sup>nd</sup> pod decreased at speed 350 m/s. So, in almost all cases, the pressure drag is more significant and pronounced at the surface of 2<sup>nd</sup> pod at all speeds.

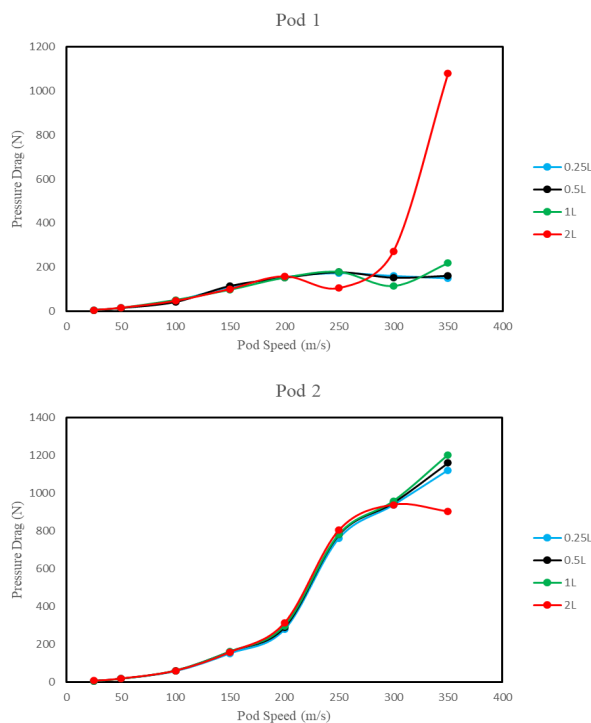


Fig. 4: Pressure Drags at Pod 1 and Pod 2

Fig. 5 shows the friction drags at the surfaces of the 1<sup>st</sup> and 2<sup>nd</sup> pods and while the speed and distance between the pods change. The friction drags at both pods clearly increase in an almost linear manner. At 1<sup>st</sup> pod, friction drags are almost nil at 25 m/s

and increase to reach almost 150 N at 350 m/s for all distance cases. Similarly, 2<sup>nd</sup> pod also starts near nil at 25 m/s and increases to about 170 N at 350 m/s. The increase in friction drag happens due to the increase of frictional forces between the fluid and the pod surface as the pod speed increases. The 2<sup>nd</sup> Pod has a slightly higher friction drag due to the increase in fluid Mach number in the region between the pods. The friction drags at the 1<sup>st</sup> pod are significant for 0.25L, 0.5L, and 1L cases because the pressure drags are low and have magnitudes similar to the friction drags. On the other hand, the 1<sup>st</sup> pod at 2L distance has a friction drag much less than the pressure drag at pod speed 350 m/s. Furthermore, the friction drags on the 2<sup>nd</sup> pod are all lower by a large margin when compared to the pressure drags, consequently it did not significantly change the total drags.

The total drag is the summation of the pressure drag and the friction drag. Fig. 6 shows the total drags at the 1<sup>st</sup> and 2<sup>nd</sup> pods under variable speed and at different distance between the pods. The trends of the lines shown are very similar and comparable to the pressure drag trends. This is because of the low friction drags compared to the pressure drags. Let et al. [14] performed a numerical study on flow induced by multiple hyperloop pods with unsteady and compressible conditions and found that the average drag (summation of total drags on 2 pods and divided by 2) is about 750 N for 2 pods at 1L and 2L. For the current case, the average total drag at 1L distance is about 700 N and is about 750 N at 2L distance. The results obtained by the current model are extremely close to the model proposed by [14], which means that there are no major changes when using unsteady conditions. The total drag that was obtained by Ho et al [3] when using one pod only was about 950 N at pod speed 300 m/s. We can see from Fig. 6 that the total drag at the 1<sup>st</sup> pod at 300 m/s is less than the total drag on a single pod model for all cases of distances between the pods. As for the 2<sup>nd</sup> pod, the total drag at 300 m/s is about 1100 N for all cases, which is higher than the single pod model. This difference in total drags between two-pod and single-pod model is due to the high friction drag at the 2<sup>nd</sup> pod which happens from the high Mach number fluid between the pods.

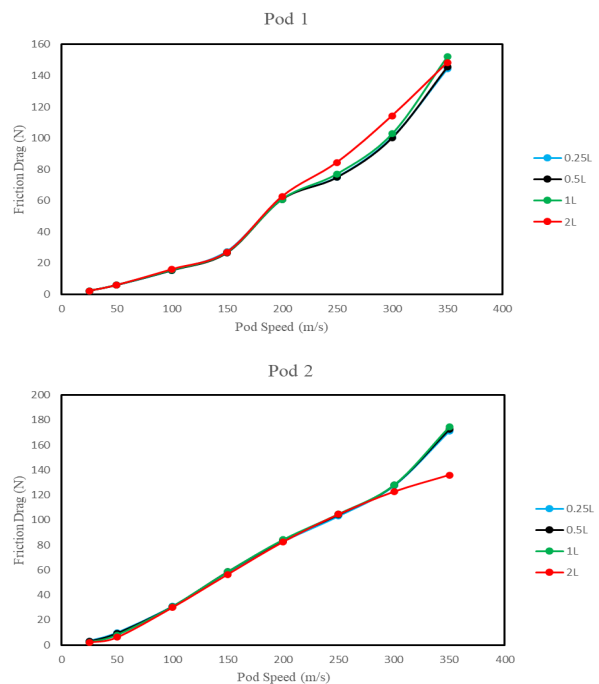


Fig. 5: Friction Drags at Pod 1 and Pod 2

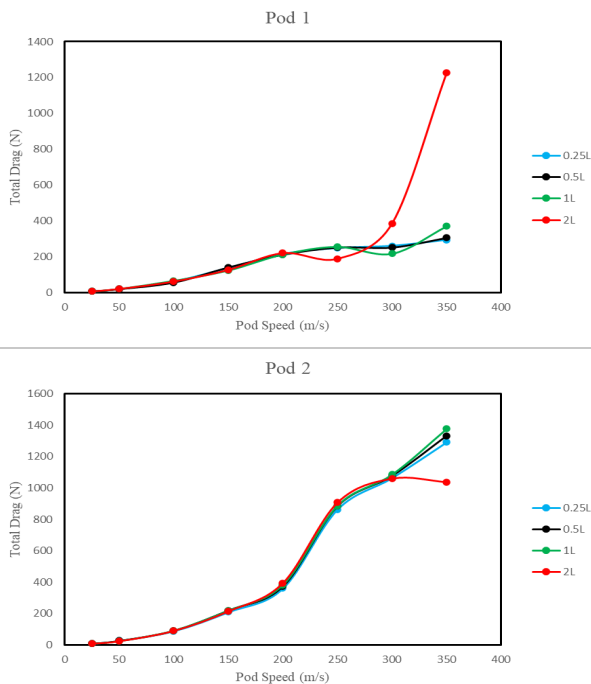


Fig. 6: Total Drags at Pod 1 and Pod 2

#### 4. Conclusion

This study involved numerically testing the performance of the flow inside a tunnel containing two hyperloop pods. The focus was obtaining the aerodynamic drag which is one of the most important parameters in the hyperloop transportation system. The effect of changing the pod speed and the distance between the two pods on the Mach number, static pressure, and aerodynamic drag were studied. To avoid choking and formation of shockwaves which can damage the hyperloop system, the flow around the pod should not exceed 1 Mach number. The results obtained showed that the flow Mach number reaches 1 at pod speed between 150 to 200 m/s. Shockwaves start appearing behind the 2<sup>nd</sup> pod at pod speed between 200 to 250 m/s. Changing the clearance distance between the 2 pods gives the same trend and the 1 Mach number flow speed occurs at the same range. Testing the pressure and the friction drag at different speeds and distances between the pods showed the following. First, for the 1<sup>st</sup> pod, the pressure drags did not significantly change when speed increased at 0.25L, 0.5L, and 1L where it was around 200 N. Second, at 2L distance between the pods, the pressure drags at pod 1 increased massively and reached about 1100 N at pod speed of 350 m/s. Third, for the 2<sup>nd</sup> pod, the pressure drags significantly increases and reached 1200 N at pod speed 350 m/s. Fourth, the friction drags at the pods were small and comparable to the pressure drags. The friction drags were much less than the pressure drag for the 2<sup>nd</sup> pod.

#### References

[1] J. Braun, J. Sousa, and C. Pekardan, "Aerodynamic design and analysis of the hyperloop," *AIAA J.*, vol. 55, no. 12, pp. 4053–4060, 2017, doi: 10.2514/1.J055634.  
 [2] M. M. J. Opgenoord and P. C. Caplan, "On the aerodynamic design of the hyperloop concept," *35th*

*AIAA Appl. Aerodyn. Conf.* 2017, no. June, 2017, doi: 10.2514/6.2017-3740.  
 [3] J. S. Oh et al., "Numerical analysis of aerodynamic characteristics of Hyperloop system," *Energies*, vol. 12, no. 3, 2019, doi: 10.3390/en12030518.  
 [4] T. T. G. Le, K. S. Jang, K. S. Lee, and J. Ryu, "Numerical investigation of aerodynamic drag and pressurewaves in hyperloop systems," *Mathematics*, vol. 8, no. 11, pp. 1–23, 2020, doi: 10.3390/math8111973.  
 [5] J. Niu, Y. Sui, Q. Yu, X. Cao, and Y. Yuan, "Numerical study on the impact of Mach number on the coupling effect of aerodynamic heating and aerodynamic pressure caused by a tube train," *J. Wind Eng. Ind. Aerodyn.*, vol. 190, pp. 100–111, Jul. 2019, doi: 10.1016/j.jweia.2019.04.001.  
 [6] J. Wang, Y. Zhang, X. Hu, P. Wang, H. Li, and Z. Deng, "Aerodynamic Characteristics of High-Temperature Superconducting Maglev-Evacuated Tube Transport," *2020 IEEE Int. Conf. Appl. Supercond. Electromagn. Devices, ASEMD 2020*, pp. 31–32, 2020, doi: 10.1109/ASEMD49065.2020.9276332.  
 [7] T. Ma et al., "Aerodynamic Drag Characteristics of the HTS Maglev Vehicle Running in a Low Air-Pressure Tube," *2020 IEEE Int. Conf. Supercond. Electromagn. Devices, ASEMD 2020*, no. 1, pp. 15–16, 2020, doi: 10.1109/ASEMD49065.2020.9276198.  
 [8] Y. Mao, M. Yang, T. Wang, F. Wu, and B. Qian, "Influence of vacuum level on heat transfer characteristics of maglev levitation electromagnet module," *Appl. Sci.*, vol. 10, no. 3, 2020, doi: 10.3390/app10031106.  
 [9] T. T. G. Le, J. Kim, M. Cho, and J. Ryu, "Effects of tail shapes/lengths of Hyperloop pod on aerodynamic characteristics and wave phenomenon," *Aerosp. Sci. Technol.*, vol. 131, p. 107962, 2022, doi: 10.1016/j.ast.2022.107962.  
 [10] A. Bose and V. K. Viswanathan, "Mitigating the piston effect in high-speed hyperloop transportation: A study on the use of aerofoils," *Energies*, vol. 14, no. 2, 2021, doi: 10.3390/en14020464.  
 [11] F. Lluésma-Rodríguez, T. González, and S. Hoyas, "Cfd simulation of a hyperloop capsule inside a low-pressure environment using an aerodynamic compressor as propulsion and drag reduction method," *Appl. Sci.*, vol. 11, no. 9, 2021, doi: 10.3390/app11093934.  
 [12] X. Hu, Z. Deng, and W. Zhang, "Effect of cross passage on aerodynamic characteristics of super-high-speed evacuated tube transportation," *J. Wind Eng. Ind. Aerodyn.*, vol. 211, no. January, p. 104562, 2021, doi: 10.1016/j.jweia.2021.104562.  
 [13] N. Nick and Y. Sato, "Computational fluid dynamics simulation of Hyperloop pod predicting laminar-turbulent transition," *Railw. Eng. Sci.*, vol. 28, no. 1, pp. 97–111, 2020, doi: 10.1007/s40534-020-00204-z.  
 [14] T. T. G. Le, J. Kim, K. S. Jang, K. S. Lee, and J. Ryu, "Numerical study of unsteady compressible flow induced by multiple pods operating in the Hyperloop system," *J. Wind Eng. Ind. Aerodyn.*, vol. 226, no. February, 2022, doi: 10.1016/j.jweia.2022.105024.  
 [15] M. Bizzozero, Y. Sato, and M. A. Sayed, "Aerodynamic study of a Hyperloop pod equipped with compressor to overcome the Kantrowitz limit," *J. Wind Eng. Ind. Aerodyn.*, vol. 218, no. October, 2021, doi: 10.1016/j.jweia.2021.104784.

